Eur. Phys. J. E **20**, 201–207 (2006)
DOI 10.1140/epje/i2005-10126-3

THE EUROPEAN PHYSICAL JOURNAL E

Effect of head-tail ratio and the range of the head-head interaction in amphiphilic self-assembly

V. Maycock and A. Bhattacharya[a]

Department of Physics, University of Central Florida, Orlando, FL 32816-2385, USA

Received 19 September 2005 and Received in final form 21 December 2005 /
Published online: 30 June 2006 –

Abstract. We investigate cluster autocorrelations, critical micelle concentration (CMC), and size distribution for amphiphiles of the type H_xT_y as a function of the amphiphilic factor $\alpha = \frac{x}{y}$ for a fixed length $l = x + y$ using a combination of reptation and kink-jump Monte Carlo (MC) moves in a two-dimensional (2D) square lattice. We find that the CMC decreases monotonically as a function of the α-parameter. For a fixed chain length l of the molecule, the symmetric molecules of the type $H_{l/2}T_{l/2}$ with $\alpha = 1$ tend to form circular micelles with relatively narrow distribution in cluster sizes. As we decrease the α-parameter to introduce head-tail asymmetry, the size distribution becomes polydisperse with occurrences of more elongated micelles. A calculation of the cluster autocorrelation function reveals that for the same chain length, symmetric amphiphiles take significantly less time to equilibrate and therefore simulation of much longer molecules is possible. Next we study the effect of the head-head repulsion term beyond next nearest neighbors. In general, the presence of a longer-range repulsive interaction reduces the average size of the micelles. We also notice that for $l = 5$, while H_2T_3 molecules produces spherical micelles, the H_1T_4 molecules($\alpha = 0.25$) often form *vesicles*. Our systematic studies bring out relevant information for controlling shapes and sizes of micelles to be used as templates in the design of self-assembled nanostructures.

PACS. 83.80.Qr Surfactant and micellar systems, associated polymers – 81.16.Dn Self-assembly – 81.16.Nd Nanolithography – 81.16.Rf Nanoscale pattern formation

Amphiphilic molecules exhibit a rich and intriguing phase behavior and offer interesting fundamental problems as well as technical challenges in soft condensed matter physics. An amphiphilic molecule contains hydrophobic (tail) and hydrophilic (head) segments linked by chemical bonds and self-assemble [1–4] into a wide variety of structures depending upon the nature of the solvent, temperature, concentration, and packing consideration, *e.g.*, geometry and volume of the head and tail segments etc. Spherical and cylindrical micelles, bi-continuous and lamellar structures, vesicles, and other phases have been observed experimentally. Theoretical [2,5,6], numerical mean-field theory [7,8], and computer simulation studies using lattice [8–24] and continuum models [25–35] have been able to reproduce some of the most important experimental results. Recent studies have also been extended to look for conditions of complete phase separation, as opposed to micellization [20,36,37], as a function of the ranges of attractive and repulsive interactions for the hydrophilic tail (T) and hydrophobic head (H) segments of the amphiphiles. Understanding self-assembling properties of amphiphilic molecules has recently become a very active field of research due to their widespread application in fabricating various devices and moieties at the nanometer length scales [38]. For example, micelle formation through the self-assembly of short hydrocarbon amphiphilic chains is used to prepare both ordered and disordered porous structures with pore sizes of the order of 40 Å [39]. Self-assembly of peptide ribbons or sheets has the potential to be used in drug delivery [40]. More recently short amphiphilic chains have been used to create a medium with evenly distributed carbon nanotubes [41]. Pattern formations of di- and tri-block copolymers are also very well known [42]. Amphiphilic self-assembly is also relevant for cell biology [43]. Cell membranes are composed of lipid bilayers which are made off amphiphilic molecules with two hydrophobic tails. The distribution of passage time of an individual polynucleotide molecule, *e.g.*, a DNA, through an ion channel in a lipid bilayer membrane has been speculated to be used for high-speed detection of sequence of bases [44]; modes translocation of a RNA or a DNA across a lipid bilayer is an important and yet unsolved problem in biophysics. The amphiphilic self-assembly has found applications in medicine as well; the pockets formed by magnetic colloids coated with phospholipid vesicles have been identified as drug

[a] e-mail: aniket@physics.ucf.edu

delivery agents [45]. It is therefore necessary to understand self-assembly in these soft-matter systems at a fundamental level.

It has been demonstrated from simple analytic arguments that the internal structure of the amphiphiles, *e.g.*, head-to-tail ratios, the polarity and effective sizes of the amphiphilic head segments etc., can dictate the final shapes of the micelles [2]. Self-consistent field theory (SCF) and single-chain mean-field theory (SCMF) have been applied to study formations by amphiphilic molecules with different degree of success [7,8]. Lattice models have been very successful to understand the micelle formation and phase separation processes of amphiphilic systems [8–22]. In previous papers [17,18] we reported specific heat and energy fluctuations in a model introduced by Care [10–13].

In this paper we study self-assembly of amphiphiles represented as H_mT_n as a function of the amphiphilic parameter $\alpha = \frac{m}{n}$. Specifically, we demonstrate how the shapes and sizes of the micelles can be controlled by varying this amphiphilic factor α for a fixed length of the amphiphile. Recently Salaniwal *et al.* [20] and Kapila *et al.* [36] following the work of Owenson and Pratt [37], have investigated conditions for micellization and phase separation in amphiphilic self-assembly as a function of the range of the interactions for hydrophilic and hydrophobic segments and derived conditions for phase separation. Our studies are complimentary to these recent investigations and demonstrates the importance of the parameter α introduced in this paper. Besides, the simulations are carried out with the aim to obtain specific useful and practical information about amphiphilic self-assembly for the fabrication of nanomaterials using self-assembled micelles, vesicles, bilayers etc., as templates. We also study the decay of the cluster autocorrelation function in this model as a function of α and make remarks about possible pitfalls in carrying out simulation in such systems. Finally, we make an important observation that a value $\alpha \simeq (0.2\text{–}0.25)$ seems favorable for *vesicle formations* when we compare our results with previous simulation studies of vesicle formation in other type, *e.g.*, double-tailed surfactants, of amphiphilic molecules [12,15].

In a 2D square lattice we denote an amphiphile as H_mT_n of length $(m+n)$ containing m hydrophilic heads (H) and n hydrophobic tails (T) connected by $m+n-1$ bonds. We use the notation *unimer* to represent each isolated amphiphile while a *monomer* represents either a head or a tail particle. N_A of such amphiphiles occupy $(m+n)N_A$ sites of a 2D square lattice of length L. The remaining $N_w = L^2 - (m+n)N_A$ sites are occupied by the solvent particles. The total energy of the system is given by

$$\mathcal{H} = \epsilon_{\rm TS} n_{\rm TS} + \epsilon_{\rm HS} n_{\rm HS} + \sum_{i=1,2,3} \epsilon^i_{\rm HH} n^i_{\rm HH} + \sum_i \epsilon^i_c. \quad (1)$$

Here $n_{\rm TS}$ and $n_{\rm HS}$ are the total number of tail-solvent (TS) and head-solvent (HS) bonds of strengths $\epsilon_{\rm TS}$ and $\epsilon_{\rm HS}$, respectively, and the term $\sum_i \epsilon^i_c$ represents the conformation energy which may include bending energies as well. We have extended the model from its original version by introducing the term $\sum_{i=1,2,3} \epsilon^i_{\rm HH} n^i_{\rm HH}$ to introduce additional repulsive head-head interaction for the 1st, the 2nd and the 3rd nearest neighbors for the head particles. The interaction energies $\epsilon_{\rm HT}$, and $\epsilon_{\rm SS}$ are set to zero. We define $\gamma = \frac{\epsilon_{\rm HS}}{\epsilon_{\rm TS}}$ ($\epsilon_{\rm TS}$ is assumed to be always positive indicating a repulsive interaction between a tail particle of the amphiphile and the solvent), $\eta_i = \frac{\epsilon^i_{\rm HH}}{\epsilon_{\rm TS}}$, and $\bar{\epsilon_i} = \frac{\epsilon_i}{\epsilon_{\rm TS}}$, and write equation (1) as

$$\mathcal{H} = \epsilon_{\rm TS} \left[n_{\rm TS} + \gamma n_{\rm HS} + \sum_i \eta_i n^i_{\rm HH} + \sum_i \bar{\epsilon}^i_c \right]. \quad (2)$$

The parameter γ is a measure of hydrophobicity and is crucial in this model. For an amphiphile of length $l = m + n$ we define amphiphilicity $\alpha = \frac{m}{n}$. The model exhibits micelle formation and contains many interesting features. Care and co-workers have studied some aspects of this model [10–13] earlier. More recently we have investigated micellar energy and size fluctuations in this model in 2D [17] and through a study of CMC in three dimensions (3D) [18].

The main purpose of this paper is to demonstrate that many of the properties of amphiphilic self-assembly, *e.g.*, CMC, distribution of cluster sizes and shapes etc., can be characterized in terms of this newly introduced parameter α. We then extend our studies to observe the effect of the head-head repulsion term η_i for $i = 1, 2$ and 3, on micellization. This term indirectly takes into account various degree of screening introduced by the solvent. Next we show that, along with the competing ranges of the range of attractive and repulsive interaction studied recently [20], the parameter α plays an important role in the context of micellization *versus* complete phase separation. We demonstrate vesicle formation in this model around $\alpha \simeq 0.25$. We notice that this might be more general than being specific to this model, as previous simulation work for double-tailed or dimeric surfactants also reports vesicle formation around $\alpha \simeq 0.25$ [15]. Finally, we emphasize that along with temperature, concentration, and chain length, the α-parameter and the repulsive factors η_i's can be used to control the shape and sizes of the micelles to be used to synthesize self-assembled nanostructures.

In studies of amphiphilic self-assembly it is important to identify the CMC as a function of temperature, chain length etc., which has been carried out by various groups using theoretical models [46–48] and simulation studies in the past including the present authors. For example, various authors find that the CMC increases with increasing temperature [18,19]. In this paper we show that *the CMC is a monotonically decreasing function of the amphiphilic factor* α. We demonstrates these results for chain lengths 6 and 5, respectively. For chain length $l = 6$, three different species are possible [49]; H_3T_3, H_2T_4, and H_1T_5 with $\alpha = 1, 0.5$, and 0.2, respectively. For chains of length 5 one can have H_2T_3, H_1T_4 with corresponding α parameter 0.67 and 0.25, respectively.

Figure 1 shows the variation of unimer concentration X_1 as a function of the total amphiphilic concentration

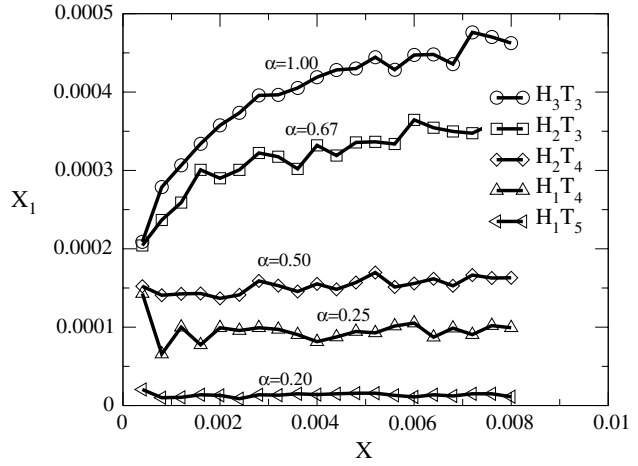

Fig. 1. Variation of the unimer concentration X_1 as a function of the total concentration X for chains with different values of α at $T = 0.6$. Notice that the CMC decreases with decreasing value of the α-parameter.

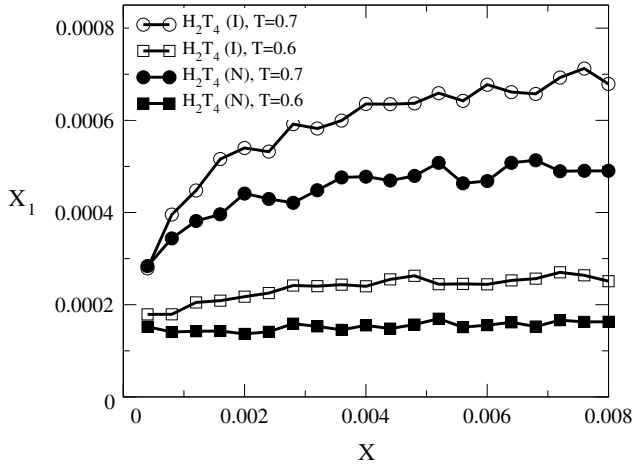

Fig. 2. Comparisons of concentration of free chains for ionic and neutral amphiphiles. The open (full) circles and squares represent temperatures 0.7 and 0.6 for ionic (neutral) amphiphiles.

X. The knee of the curve roughly identifies the critical micelle concentration (CMC). Beyond this concentration X_1 does saturate, as free energetically it becomes increasingly favorable to the formation of larger clusters. Notice that even for chains of two different lengths, the plot of X_1 as a function of X shows a systematic variation as a function of α. The CMC is minimum for H_1T_5 ($\alpha = 0.2$) and then becomes larger for H_1T_4, H_2T_4, H_2T_3, and H_3T_3 with α values 0.25, 0.50, 0.67, and 1.0, respectively. We notice that CMC *increases monotonically as a function of* α. Previous studies of amphiphilic self-assembly do not emphasize the role of the amphiphilic factor α.

Next we consider the effect of the head-head repulsion terms η_1, η_2, and, η_3 on the CMC. These terms take into account a different degree of screening for amphiphiles with ionic heads. We will loosely call these amphiphiles with additional head-head interactions as *ionic* amphiphiles, reserving the name *neutral* for those where η_i's are set to zero. Figure 2 shows the difference that arises from the introduction of additional 2nd (n2) and 3rd (n3) head-head next nearest neighbors, shown for H_2T_4 at two different temperatures, $T = 0.7$ and $T = 0.6$. Two things can be deciphered from this plot: i) for the same chain length l and amphiphilic factor α, ionic amphiphiles show a saturation at a larger value of X_1 and further along X; ii) it is also evident that the introduction of a longer-range interaction increases the effective temperature of the system. We have checked that this is a generic feature as we find the same results in our off-lattice simulation studies [50].

We have studied the effect of α, η_1, η_2, and η_3 on the cluster distribution of micelles for concentrations much larger than the CMC. For larger concentrations, when clusters begin to form, it is important to know how the cluster autocorrelation decays as a function of MC steps, in order to take a statistical average of cluster distributions. The tracer autocorrelation function $A(t)$ is defined as

$$A(\tau) = \frac{\langle N(t+\tau)N(t)\rangle - \langle N(t)\rangle^2}{\langle N^2(t)\rangle - \langle N(t)\rangle^2}\,, \qquad (3)$$

where, for a given τ, the averages $\langle\cdot\cdot\rangle$ are taken over all the chains in the system and for all possible time t. Here $N(t)$ is the size of the micelle where a tracer chain resides at time t. This function has been used by Haliloglu and Mattice [51], and by Hatton, co-workers [16,28], and by the present authors [35] to estimate the length of the time interval τ_c that the system needs to evolve from one statistically independent configuration to another. It is important to know τ_c to collect data for statistical averaging purposes and to estimate the total length of the simulation time after the system has equilibrated. By definition, $A(0) = 1$, it is expected to decay to zero at late time. We choose τ_c to be the time when $A(\tau)$ decays to 0.2. Typically we have run the simulation for (300–500)τ_c. Previous MC studies [16,51] and a stochastic MD study [28] concentrated on symmetric amphiphiles where the length of the hydrophobic and hydrophilic segments is the same (H_xT_x in our notation). Here we study the behavior $A(t)$, as a function of MC steps t, for different α's and compare the results with those for nonzero values of η_i's.

For concentrations X of the amphiphiles which are below the CMC, $A(\tau)$ increases with X; but for X beyond CMC, $A(\tau)$ decreases with increasing X. For larger concentrations, the average distance between the clusters is less and the diffusion of chains from one cluster to the other happens at a faster rate. This results in a rapid decrease of $A(\tau)$. Figure 3 shows $A(t)$ as a function of temperature for H_2T_4. The correlation increases very rapidly when the temperature is decreased from 0.7 to 0.5. The same figure shows the effect of the head-head repulsion term. The head-head repulsing term makes the cluster autocorrelation decay faster for the same amphiphiles. We have checked that the trend is the same for all the amphiphiles. Figure 4 shows the variation of $A(\tau)$ as a function of the total concentration X. Our choices of concentrations $X = 1\%, 2\%$, and 3% are all beyond the CMC

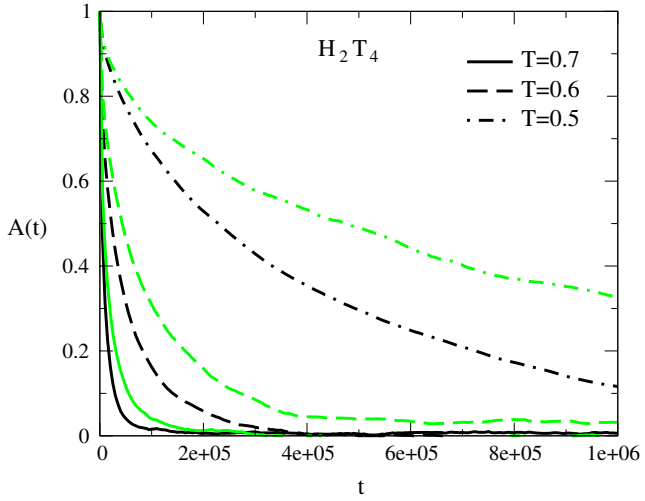

Fig. 3. (Colour on-line) Variation of the autocorrelation function $A(t)$ as a function of different temperatures for H_2T_4 at concentration $X = 0.03$. The light (green) and dark (black) lines represent neutral and ionic amphiphiles, respectively.

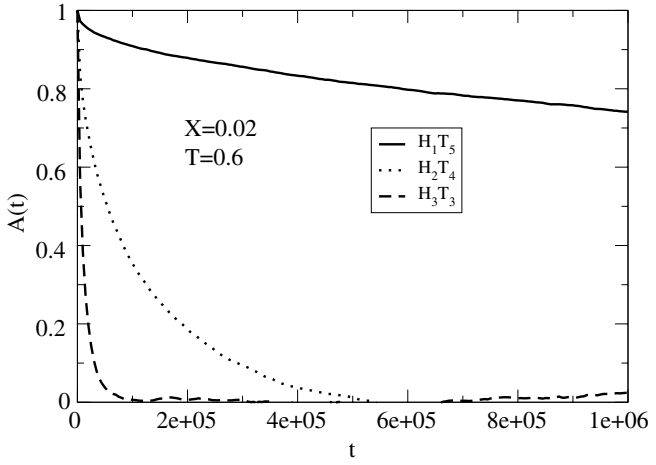

Fig. 5. Variation of the autocorrelation function $A(t)$ as a function of the amphiphilic factor α for H_3T_3 ($\alpha = 1.0$), H_2T_4 ($\alpha = 0.5$), and H_1T_5 ($\alpha = 0.2$) at temperature $T = 0.6$. $A(t)$ has the fastest decay for the largest value of α.

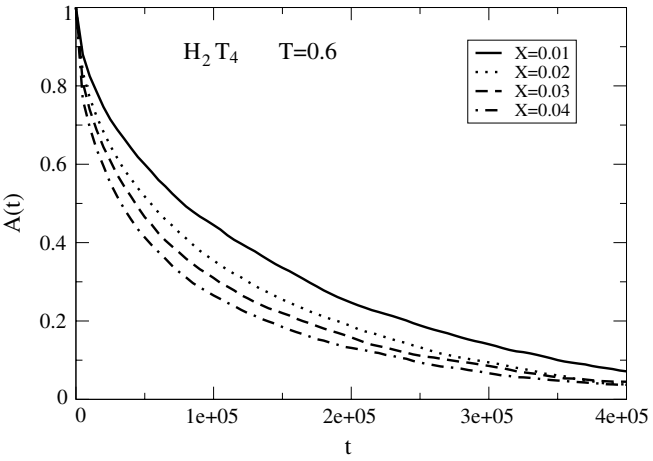

Fig. 4. Variation of the autocorrelation function $A(t)$ as a function of different concentrations for H_2T_4 at temperature $T = 0.6$.

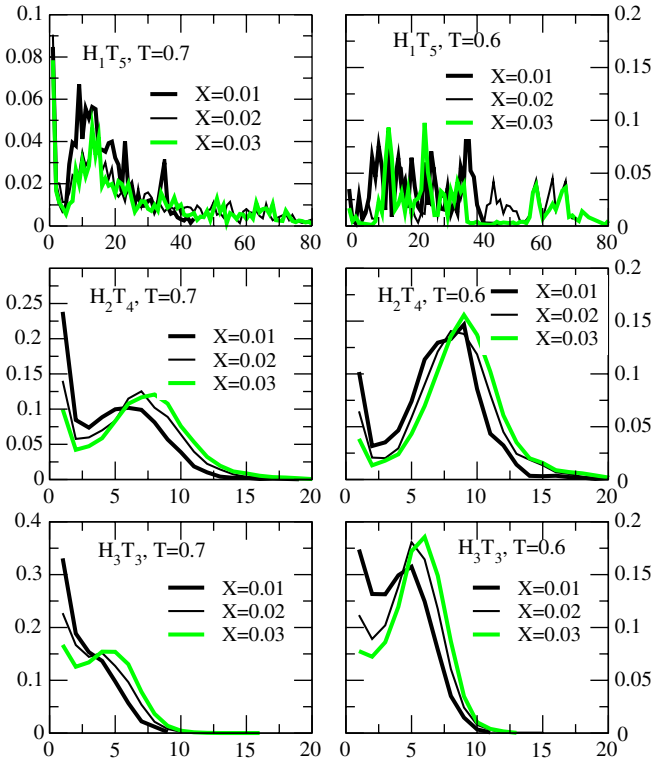

Fig. 6. (Colour on-line) Cluster distribution for neutral H_1T_5 ($\alpha = 0.5$), H_2T_4 ($\alpha = 1.0$), and H_3T_3 ($\alpha = 0.2$) for concentrations 0.01 (thick black), 0.02 (thin black), and 0.03 (thick green) at temperatures $T = 0.7$ (left) and $T = 0.6$ (right), respectively. The amphiphilic factor α has a marked impact on the cluster size.

at this particular temperature. We notice that $A(\tau)$ decreases at larger concentration.

Finally, we show the influence of the amphiphilic geometry on $A(\tau)$ in Figure 5. Notice that for H_3T_3 with $\alpha = 1$, the autocorrelation has the fastest decay. It has the largest head group area for a fixed chain length. As the head-tail ratio is decreased the autocorrelation $A(t)$ for H_2T_4 ($\alpha = 0.5$) and H_1T_5 ($\alpha = 0.2$) increases significantly. This behavior could be inferred from Figures 1 and 2. We observe from Figures 1 and 2 that an amphiphile with larger head can be looked at as an amphiphile with a smaller head at a higher temperature. That $A(\tau)$ decays faster at a higher temperature (Fig. 3) would also imply a faster decay for large-head amphiphiles as shown in Figure 5. We have used the correlation function to determine the MC time interval to collect data for statistical averaging purposes. Data is taken at MC time intervals bigger than τ_c.

It is worth noticing that it is meaningless to run simulation for H_1T_5 at $T = 0.5$ as $t_c \to \infty$ for all practical purposes. Therefore, it is very important to calculate $A(t)$ for various interaction parameters even for short-chain amphiphiles.

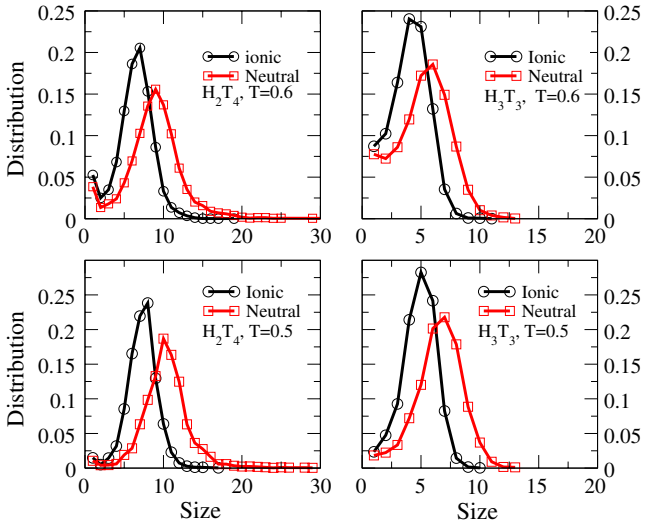

Fig. 7. Cluster distribution for H_2T_4, and H_3T_3 for concentration 0.03 at temperatures $T = 0.6$ and $T = 0.5$. The circles and the squares represent ionic and neutral amphiphiles, respectively.

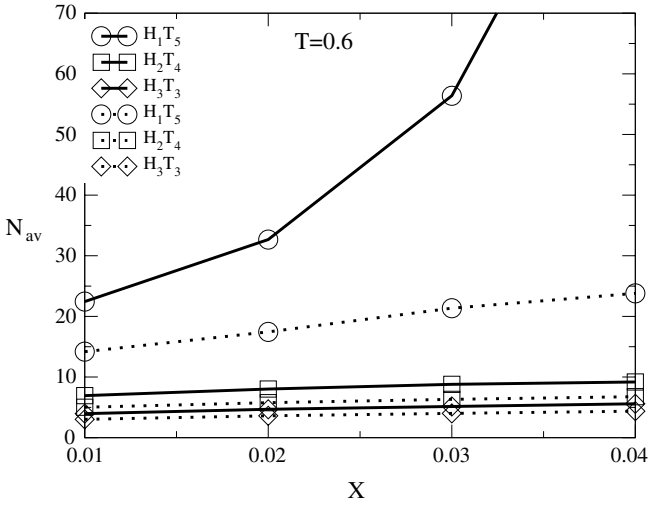

Fig. 8. Average cluster size as a function of total amphiphilic concentration X for H_1T_5 (circles), H_2T_4 (squares), and H_3T_3 (diamonds) at temperature $T = 0.6$. The solid and the dotted lines represent neutral and ionic amphiphiles, respectively.

The computational time for the results reported in this paper is equivalent to running a Pentium-IV 2.0 GHz processor Linux box continuously for about 70 days.

During the simulation we have monitored the cluster distribution ($\frac{X_n}{n}$) for several different concentrations and temperatures for various amphiphiles H_mT_n with $m + n = 5$ and 6, respectively. Specifically, we have addressed the effects of the amphiphilic parameter α and that of the head-head repulsion terms η_1, η_2 and η_3. Figure 6 shows the cluster distribution for H_1T_5, H_2T_4, and H_3T_3 ($\alpha = 0.5$, 1.0, 0.2, respectively). It is evident from Figure 6 that as α increases not only the average size of the cluster decreases, but the distribution becomes sharper for larger values of α. This demonstrates that by tuning the α-parameter, micelles of a desired size can be obtained without changing the length of the amphiphile. Finally, we show the effect of the head-head interaction on cluster distribution. An additional interaction among the heads keeping all other parameters unchanged favors the formation of smaller clusters with a sharper distribution as shown in Figure 7. This result combined with the the knowledge of the amphiphilic factor α will guide the synthesis of micelles of a given size. In a recent interesting study Salaniwal, Kumar, and Panagiotopoulos [20] have looked into the competing range of attractive and repulsive interactions in a lattice model of micellization using histogram-reweighting Gibbs ensemble method. Their conclusion that the range of the attractive interaction has to be comparable to or smaller than the range of the repulsive interaction to facilitate micelle formation is consistent with our observation. In our studies we have monitored the average cluster size, specifically above the CMC. Figure 8 shows the variation of the average cluster size as a function of α, both for neutral and ionic amphiphiles. For H_3T_3 ($\alpha = 1.0$) and H_2T_4 ($\alpha = 0.5$), the average cluster size is practically insensitive to the total concentration, *i.e.*, they exhibit micellization. However, for H_1T_5 with $\alpha = 0.2$, the average cluster size seems to diverge for the neutral amphiphiles, while for the ionic amphiphiles, the presence of the additional repulsive terms significantly suppresses the growth. Therefore, it is possible to interpolate between micellization and complete phase separation by solely varying the α-parameter, keeping the strength and the range of interactions the same [36]. It will be worthwhile to extend the work of Salaniwal *et al.* and study phase separation *versus* micellization as a function of both α as well as the range of the competing interactions.

Along with nearly spherical and elongated micelles, we have also observed rather long-lived vesicles from the movies made from the stored co-ordinates obtained during simulation. We have noticed that the H_1T_4 molecules at 15% volume fraction ($\alpha = 0.25$) during the self-assembly form vesicles whose lifetime is quite long (see Fig. 9). It is interesting to note that Brindle and Care [12] have also noticed vesicle formation in three dimensions for H_1T_5 ($\alpha = 0.20$) at 10% volume fraction. Bernardes [15] have also observed spontaneous vesicle formation in two-tailed surfactants of total length 12. The α value of this dimeric surfactant is surprisingly close to 0.25. It is therefore worthwhile to explore spontaneous vesicle formation in the vicinity of $\alpha \sim 0.2$–0.25 for other chain lengths in two- and three-dimensional lattice simulations. It is also interesting to note that analytical studies using free-energy expansion in terms of curvature tensors [3,52,53] predict instability of a bilayer membrane for $\alpha = 0.2$.

To summarize, we have studied the self-assembly of amphiphilic molecules represented as H_xT_y as a function of the amphiphilic factor $\alpha = \frac{x}{y}$ for a fixed length $l = x+y$. Although there have been many studies of amphiphilic self-assembly both in lattice and continuum models this issue has not been properly emphasized in the past. We have been able to demonstrate that it is useful to characterize

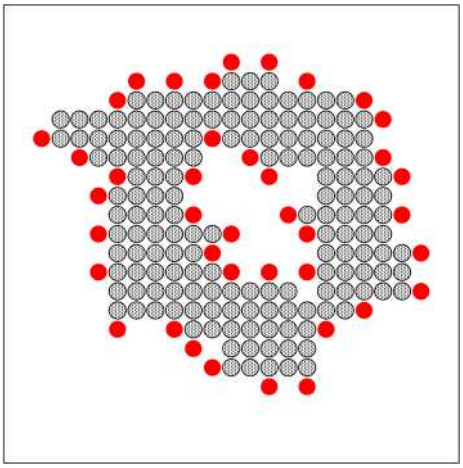

Fig. 9. Vesicle formation at 3% concentration of H_1T_4 (15% volume fraction) at $T = 0.6$. The vesicle is stable for 10^5 MC steps and changes shape.

different aspects of self-assembly, *e.g.*, the CMC, cluster autocorrelations, size distributions, etc., as a function of the parameter α. These quantities which characterize micellization show a systematic variation as a function of α. For example, CMC is a monotonically increasing function of α. The shape of the cluster distribution is also a strong function of α. For $\alpha \sim 1.0$ the cluster distribution is narrow and sharply peaked, whereas for $\alpha = 0.2$ the distribution is flat and polydispersed. Our results are in accord with recent SANS experiments [54] on n-alkyl polyglycol ether C_iE_j-type surfactants.

The cluster autocorrelations are smallest for the largest value of α. While for $0.5 < \alpha < 1$ we observe spherical micelles, for $\alpha = 0.25$ we have seen long-lived vesicles during simulation. It is worth mentioning that in the simulation studies of Bernardes [15] the α value for the dimeric surfactants with which they observed vesicular structures is also close to 0.25. Therefore, we believe that this information can help to construct analytic arguments for vesicle formation. A thorough understanding of vesicle formation may have potential benefit in the biotechnological industry as synthetic biocompatible vesicles can be used as carriers of drugs. We have also incorporated the screened Coulomb interaction for the charged head groups by introducing head-head interactions up to the third nearest neighbors. A comparison shows that a longer-range repulsion produces more compact clusters and raises the effective temperature. It is also evident that the presence of a long-range head-head interaction limits the size of the micelles and suppresses phase separation. Therefore, by tuning the range of the interaction and the amphiphilic factor it is possible to design array of micelles of a desired size and periodicity. This may have important bearing on nanotechnology.

It is worth making a comparison of our results with recent relevant studies and comment on the possible future direction of our work.

Kapila *et al.* [36] in a model similar to ours have been able to study relatively longer chain molecules H_1T_{12} ($\alpha = 0.08$) and H_7T_{12} ($\alpha = 0.58$). That H_1T_{12} does not form a micelle is consistent with our way of characterization with the α-parameter. Amphiphiles with such a small value of $\alpha = 0.08$ tend to phase separate while H_7T_{12} with $\alpha \sim 0.6$ form micelles. In carrying out MC simulation, in addition to the usual reptation and kink-jump moves, Kapila *et al.* used cluster moves as well. It is expected that these cluster moves will introduce faster cluster-cluster fusions or fragmentations into smaller clusters. As a result, the autocorrelation will decay faster allowing MC studies of much longer amphiphilic molecules.

Our studies share similarities with some of the lattice MC work done earlier [7,8,24]. However, we consider three distinct types of molecules: head (H), tail (T), and solvent (S) molecules explicitly unlike many previous studies where the elementary blocks of the hydrophilic segments are the same as the solvent molecules. As a result, we have been able to introduce H-H repulsion which goes up to the 3rd nearest neighbor and find that the range of the interaction has a marked effect on the cluster size distribution. Besides, extracting features in terms of the amphiphilic parameter α and the range of the interaction is important to understand the generic aspects of amphiphilic self-assembly. For critical micelle concentration, such an attempt has been made by Rodriguez-Guadarrama *et al.* where they have established a relation between model parameters and real experiments [24].

We would like to make some remarks about the theoretical studies of curvature-induced instability of diblock copolymer bilayers [3,52,53]. For a copolymer consisting of length $N_A + N_B$, under strong segregation limit, the free energy F_s due to Wang [52] is

$$F_s = f^* \left\{1 + [-(2/15) + (9/10)\phi - (2/5)\phi^2]\bar{c}^2 + \right\},$$

where $\phi = N_A/(N_A+N_B)$, f^* is the minimized free energy per chain for a monolayer in the flat geometry, and $\bar{c}$ is the dimensionless curvature, respectively. Wang notices from the above expression that for $\phi < 0.16$ the coefficient of the quadratic term becomes negative indicating that the flat bilayer becomes unstable with respect to spherical deformation. Although, one may wonder if this analysis is applicable to very short chains, we note that the value $\phi = \frac{N_A}{N_A+N_B} \sim 0.16 \sim \frac{1}{6}$, (in our notation $\alpha = \frac{N_A}{N_B} = \frac{1}{5} = 0.2$) is close to the values for which spherical vesicles are observed in simulation.

Currently we are looking at chain molecules of different lengths which are an integral multiple of each other, *e.g.* H_nT_m, $H_{2n}T_{2m}$, etc., with the same value of α using the additional MC moves beyond reptation and kink-jump. We are also introducing additional potentials among different segments of the amphiphilic molecules with the aim to understand the relationship between the structure of micelles with the nature of the interaction potentials. These investigations are currently under progress and will be reported in a future paper.

The research reported here is supported in part by a grant from the National Science Foundation (NSF) NIRT (ENG/ECS and CISE/EIA # 0103587) grant. We thank Kevin Belfield, Weili

Luo, and Geuorgui Bourov for various discussions. V. Maycock was partially supported by a FGAMP fellowships. We thank Varol Kaptan and Sergio Tafur for technical assistance.

References

1. V. De Giorgio, M. Corti (Editors), *Physics of Amphiphiles: Micelles, Vesicles and Microemulsions* (North-Holland, 1985).
2. J.N. Israelachvili, *Intermolecular and Surface Forces* (Academic, New York, 1985).
3. S.A. Safran, *Statistical Thermodynamics of Surfaces, Interfaces, and Membranes* (Addison Wesley, New York, 1994).
4. R.G. Larson, *The Structure and Rheology of Complex Fluids* (Oxford University Press, 1999).
5. D. Blankschtein, G.M. Thurston, G.B. Benedek, Phys. Rev. Lett. **54**, 955 (1985); G.M. Thurston, D. Blankschtein, M.R. Fisch, G.B. Benedek, J. Chem. Phys. **84**, 4558 (1986); D. Blankschtein, G.M. Thurston, G.B. Benedek, J. Chem. Phys. **85**, 7268 (1986); S. Puvvada, D. Blankschtein, J. Chem. Phys. **92**, 3710 (1990).
6. A. Ben-Shaul, I. Szleifer, W.M. Gelbart, J. Chem. Phys. **83**, 3597 (1985); I. Szleifer, A. Ben-Shaul, W.M. Gelbart, J. Chem. Phys. **83**, 3612 (1985).
7. C.M. Wijmans, P. Linse, Langmuir **11**, 3748 (1995).
8. A.D. Mackie, A.Z. Panagiotopoulos, I. Szleifer, Langmuir **13**, 5022 (1997).
9. R.G. Larson, L.E. Scriven, H.T. Davis, J. Chem. Phys. **83**, 2411 (1985); R.G. Larson, J. Chem. Phys. **89**, 1642 (1988); **91**, 2479 (1989); **96**, 7904 (1992); J. Phys. II **6**, 1441 (1996).
10. C.M. Care, J. Phys. C **20**, 689 (1987).
11. C.M. Care, J. Chem. Soc. Faraday Trans. **83**, 2905 (1987).
12. D. Brindle, C.M. Care, J. Chem. Soc. Faraday Trans. **88**, 2163 (1994).
13. J.-C. Desplat, C.M. Care, Mol. Phys. **87**, 441 (1996).
14. A.T. Bernardes, V.B. Henriques, P.M. Bisch, J. Chem. Phys. **101**, 645 (1994).
15. A.T. Bernardes, J. Phys. II **6**, 169 (1996).
16. P.H. Nelson, G.C. Rutledge, T.A. Hatton, J. Chem. Phys. **107**, 10777 (1997).
17. Aniket Bhattacharya, S.D. Mahanti, J. Phys.: Condens. Matter **12**, 6141 (2000).
18. Aniket Bhattacharya, S.D. Mahanti, J. Phys.: Condens. Matter **13**, L861 (2001).
19. A. Floriano, E. Caponetti, A.Z. Panagiotopoulos, Langmuir **15**, 3143 (1999).
20. S. Salaniwal, S.K. Kumar, A.Z. Panagiotopoulos, Langmuir **19**, 5164 (2003).
21. C.S. Shida, V.B. Henriques, J. Chem. Phys. **115**, 8655 (2001).
22. A. Milchev, Aniket Bhattacharya, K. Binder, Macromolecule **6**, 1881 (2001).
23. D. Viduna, A. Milchev, K. Binder, Macromol. Theory Simul. **7**, 649 (1998).
24. L.A. Rodriguez-Guadarrama, S.K. Talsania, K.K. Mohanty, R. Rajagopalan, Langmuir **15**, 437 (1999).
25. D.R. Rector, F. van Swol, J.R. Henderson, Mol. Phys. **82**, 1009 (1994).
26. B. Smit, K. Esselink, P.A. Hilbert, N.M. van Os, L.A.M. Rupert, I. Szleifer, Langmuir **9**, 9 (1993); B. Smit, P.A. Hilbert, K. Esselink, L.A.M. Rupert, N.M. van Os, J. Chem. Phys. **95**, 6361 (1991).
27. B. Palmer, J. Liu, Langmuir **12**, 746; 6015 (1996).
28. F.K. von Gottberg, K.A. Smith, T.A. Hatton, J. Chem. Phys. **106**, 9850 (1997).
29. R. Goetz, R. Lipowsky, J. Chem. Phys. **108**, 7397 (1998).
30. A. Bhattacharya, A. Chakrabarti, S.D. Mahanti, J. Chem. Phys. **108**, 10281 (1998).
31. J.-B. Maillet, V. Lachet, P.V. Coveney, Phys. Chem. Chem. Phys. **1**, 5277 (1999).
32. T. Soddemann, B. Dunweg, K. Kremer, Eur. Phys. J. E **409**, 409 (2001).
33. S. Bogusz, R.M. Venable, R. Pastor, J. Phys. Chem. **105**, 8312 (2001).
34. P.K. Maiti, Y. Lansac, M.A. Glaser, N.A. Clark, Y. Rouault, Langmuir **18**, 1908 (2002).
35. G. Bourov, Aniket Bhattacharya, J. Chem. Phys. **119**, 9219 (2003).
36. V. Kapila, J.M. Harris, P.A. Deymer, S. Raghavan, Langmuir **18**, 3728 (2002).
37. B. Owenson, L.R. Pratt, J. Phys. Chem. **88**, 2905 (1984).
38. Z. Zhang, M.A. Horsch, M. Lamm, S.C. Glotzer, Nano Lett. **3**, 1341 (2003).
39. C.T. Kresge, M.E. Leonowicz, W.J. Roth, J.C. Vertuli, J.S. Beck, Nature **359**, 710 (1992); P.T. Tanev, T.J. Pinnavaia, Science **267**, 865 (1995); K.M. McGrath, D.M. Dabs, N. Yao, I.A. Aksay, S.M. Gruner, Science **277**, 552 (1997).
40. H. Matsui, J. Phys. Chem. B **104**, 3383 (2000).
41. B. Vigolo, A. Penicaud, C. Coulon, C. Sauder, R. Pailler, C. Journet, P. Bernier, P. Poulin, Science **290**, 1331 (2000).
42. F.S. Bates, G.H. Fredrickson, Phys. Today **52**, 32 (1999).
43. B. Alberts *et al.*, *Molecular Cell Biology*, 4th ed. (Garland Science, New York, 2002).
44. J.J. Kasianowicz, E. Brandin, D. Branton, D. Deamer, Proc. Natl. Acad. Sci. U.S.A. **93**, 13770 (1996); A. Meller, L. Nivon, E. Brandin, J. Golovchenko, D. Branton, Proc. Natl. Acad. Sci. U.S.A. **97**, 1097 (2000).
45. C. Sangregorio, J.K. Wiemann, C.J. O'Connor, Z. Rosenzweig, J. Appl. Phys. **85**, 5699 (1999).
46. W. Wenzel, C. Ebner, C. Jayaprakash, R. Pandit, J. Phys. C **1**, 4245 (1989).
47. E. Ruckenstein, R. Nagarajan, J. Phys. Chem. **79**, 2622 (1975); R. Nagarajan, E. Ruckenstein, Langmuir **7**, 2934 (1980).
48. A. Ben-Naim, F.H. Stillinger, J. Phys. Chem. **84**, 2872 (1980); F.H. Stillinger, A. Ben-Naim, J. Chem. Phys. **74**, 2510 (1981).
49. We restrict ourselves to the case where the number of head monomers is less than or equal to the number of tail monomers.
50. K. Kitanovski, G. Bourov, A. Bhattacharya, unpublished.
51. T. Haliloglu, W.L. Mattice, Chem. Eng. Sci. **49**, 2851 (1993).
52. Z. Wang, Macromolecules **25**, 3702 (1992).
53. A. Adjari, L. Leibler, Macromolecules **24**, 6803 (1991).
54. O. Glatter, G. Fritz, H. Lindner, J. Brunner-Popela, R. Mittelbach, R. Strey, S.U. Egelhaaf, Langmuir **16**, 8692 (2000).